International Journal of Pavement Engineering

ISSN: (Print) (Online) Journal homepage: https://www.tandfonline.com/loi/gpav20

Discomfort limits provided by railroad crossings to passenger cars

Ufuk Kırbaş & Mustafa Karaşahin

To cite this article: Ufuk Kırbaş & Mustafa Karaşahin (2021): Discomfort limits provided by railroad crossings to passenger cars, International Journal of Pavement Engineering, DOI: 10.1080/10298436.2021.2001817

To link to this article: https://doi.org/10.1080/10298436.2021.2001817

INTERNATIONAL JOURNAL OF PAVEMENT ENGINEERING
https://doi.org/10.1080/10298436.2021.2001817

Taylor & Francis
Taylor & Francis Group

Discomfort limits provided by railroad crossings to passenger cars

Ufuk Kırbaş[a] and Mustafa Karaşahin[b]

[a]Department of Civil Engineering, Ondokuz Mayis University, Samsun, Turkey; [b]Department of Civil Engineering, Istanbul Gelisim University, Istanbul, Turkey

ABSTRACT

Railroad crossings occupy an important place in the transport network and human life in urban transport networks that develop due to increasing urban populations. A railroad crossing is a type of pavement distress accepted by the authorities due to its direct effect on ride comfort. The study determined the level of discomfort that passenger cars are exposed to at railroad crossings. In this context, vibration measurements were made at different speeds on-road profiles with known geometries with a passenger car. The vibration data recorded within the scope of the study was characterised and evaluated using the weighted root-mean-square acceleration (a_w) parameter defined in ISO 2631 standard. With the help of these data, a vehicle dynamic model was calibrated, and vehicle responses were digitised. Subsequently, vibration data were recorded from railroad crossings with different distress severities: low, medium, and high at different ride speeds. By comparing the vibration data, the compliance of railroad crossings with the road classifications accepted in the ISO 8608 standard was investigated. This modelling determined the levels of discomfort that a person riding in a passenger car is exposed to on passages double-track and single-track railroad crossings at different ride speeds within the city.

ARTICLE HISTORY
Received 7 August 2021
Accepted 30 October 2021

KEYWORDS
Railroad crossing; ride comfort; pavement distress; vehicle vibration; discomfort limit

1. Introduction

As a result of developing urbanisation, transportation networks have to grow more and more every day. Nevertheless, in today's modern cities, rail transport emerges as an indispensable form of transportation in public transportation. As a result of the development, the increase in the intersection of highway and railroad networks in urban development is inevitable. The level of service in a highway section is expressed by taking into account each of the principles of being smooth, comfortable, and safe separately. In the event, ride quality is defined as the degree of the total experience that occurs, taking into account the mobility environment and other factors felt by the driver and passengers in a journey (Griffin 2007, Kırbaş and Karaşahin 2018b). The most important reason affecting discomfort while riding is the pavement distresses observed on the road surface. Railroad crossing, which is one of twenty different types of pavement distress according to ASTM D 6433 standard (ASTM 2016), emerges as a component that reduces ride comfort, especially in urban road transport networks.

A large number of indexes have been developed to numerically express the current performance of road pavements. Although International Roughness Index (IRI), Pavement Condition Index (PCI), Pavement Serviceability Index (PSI), Ride Number (RN) are among the main ones, it is known that there are many more indexes (Kırbaş and Karaşahin 2016). It is a well-known fact that the most important effect in determining pavement performances and also ride comfort is the distresses and defects seen in the pavements (Haas *et al.* 1994, Kırbaş and Karaşahin 2018a). To numerically express ride comfort, the frequency-weighted vibration assessment (a_w) mentioned in the ISO 2631 standard is often used (ISO 1997). In addition, the Vibration Dose Value (VDV) parameter is also preferred, although not very often (ISO 1997, Griffin 2007, Cantisani and Loprencipe 2010, Griffin 2012, Kırbaş and Karaşahin 2018b, Múčka 2020).

It is noteworthy that there are numerous studies in the literature investigating the relationship between vibration exposed within the vehicle and pavement performance indexes. In the studies carried out, ride comfort is analysed with the help of dynamic vehicle models that react to signal stacks representing macrotexture depth, in other words, according to profile inputs that can express the road surface numerically. Cantisani and Loprencipe (2010) have created a dynamic vehicle model, calibrated it with road acceleration measurements that they can determine the road profile. They calculated IRI and vertical a_w values with the help of the dynamic vehicle model they calibrated using Long-Term Pavement Performance (LTPP) data, and as a result of their analysis, they proposed IRI thresholds for ride comfort. Similarly, Zhang *et al.* (2020) compared IRI and a_w by simulating the road surface and profile in a vehicle driving simulator. In the study in which driver subjects of different ages and education levels were also evaluated, IRI comfort threshold values were proposed. Hou *et al.* (2009) evaluated the relationships between IRI and aw values produced utilising a dynamic vehicle model in their studies.

Besides, studies evaluating ride comfort with artificial road profiles produced according to the road classes defined in the ISO 8608 standard (ISO 1995, Du *et al.* 2020) also draw attention in the literature. Nguyen *et al.* (2019) researched the

CONTACT Ufuk Kırbaş ufuk.kirbas@omu.edu.tr, ufukkirbas@gmail.com

similarities between the IRI and ride comfort produced by a dynamic model representing the urban passenger bus, and developed IRI comfort thresholds for bus-type vehicles. In the dynamic vehicle model calibrated by field measurements, the road class thresholds recommended in ISO 8608 were used as input and IRI values corresponding to the road categories were determined. Agostinacchio *et al.* (2013) evaluated the vehicle loads in the passenger car, bus, and truck dynamic vehicle model of five different road profiles defined in ISO 8608. In his study, Múčka (2015) analysed the effects on driving comfort by adding a crack-like signal to the road profiles produced according to ISO 8608 on rigid road pavements.

Likewise, the relationships between pavement performance and vibration measurements made on-road sections of certain lengths where pavement superimposed distress were investigated (Wang and Easa 2016, Abudinen *et al.* 2017, Múčka 2017, 2021). In repeated measurements at diverse ride speeds, IRI is mostly used as the pavement performance evaluation index, as well as indexes such as PSI and RN are preferred (La Torre *et al.* 2002, Yu *et al.* 2006, Fuentes *et al.* 2021). It is understood that PCI is preferred in urban road pavements (Kırbaş and Karaşahin 2018a, 2019). It is noteworthy that only the vibrations in the vertical direction are evaluated quite intensively in the analyses. The frequency-weighted vibration parameter (a_w), sometimes the VDV parameter, is used to express ride comfort (Kırbaş and Karaşahin 2018b, Múčka 2020). Also, approaches using statistical parameters such as root mean square (RMS), power spectral density (PSD) (Zhang and Yang 2010), RMS for vertical acceleration (Muniz de Farias and de Souza 2009, Guanyu *et al.* 2020), jolt (sudden shock) (Yu *et al.* 2006), a root-mean-square of the successive differences (RMSSD) (Zhang *et al.* 2020) can be seen to express vibration numerically (Múčka 2015). It is seen that linear deterministic modelling approach is frequently used in determining the relationships between parameters, as well as approaches such as exponential, probabilistic, artificial neural network and fuzzy logic. In the studies, it is emphasised that the vibrations recorded in passenger car type vehicles of different sizes, especially at urban speed limits, do not vary significantly depending on the brand and model of the vehicle (Duarte and de Melo 2018, Múčka 2020, 2021).

Researchers have chosen to evaluate vibration measurements made with smartphone technology, thinking that it can be a very cheap and feasible solution in determining the effects of road pavement on vehicles (Guanyu *et al.* 2020, Janani *et al.* 2020). Presently, as a result of significant achievements in sensor capabilities in smartphone technology, by using high-sensitive vibration measurements, the locations of distresses such as pothole, patch, bump, which negatively affect riding can be detected (Bridgelall 2015, Janani *et al.* 2020). Besides, driving manoeuvers such as sudden braking or sudden acceleration can also be detected and information about trip comfort can be collected (Sauerwein and Smith 2011, Astarita *et al.* 2012, Vittorio *et al.* 2014, Bridgelall 2015).

In studies on the subject, it is seen that the effects of vibrations originating from the surface of the pavement exposed in the vehicle on the ride comfort are often made utilising performance index components (IRI, PCI, etc.) that express the current state of the pavement, frequently. However, there are quite a limited number of studies that can reveal the effects of road distress, which is frequently encountered by drivers in urban road networks, on discomfort individually.

In this study, the levels of discomfort that the drivers and passengers travelling in passenger car type vehicles, which are the most common in urban road traffic, are affected by railroad crossings at diverse speeds are analysed. A quarter-car dynamic vehicle model was created in Simulink (Matlab ®) environment to make the analysis. To calibrate the vehicle model, vibration measurements in the range of 20–50 km/h were made with a passenger car type vehicle on the road sections where there are bumps at two different heights. The vibration data recorded within the scope of the study were characterised and evaluated with the help of the frequency-weighted root-mean-square acceleration (a_w) parameter defined in the ISO 2631 standard. Road profiles created with parameters appropriate to the road classifications accepted in the ISO 8608 standard were used as inputs to the dynamic vehicle model. The differences between the real vibration measurements and the dynamic simulation results were calibrated, enabling the dynamic vehicle model to give results close to field measurement data on a specified road profile. Afterward, vibration data were recorded from railroad crossings with three different distress severities as Low (L), Medium (M), and High (H) specified in ASTM D 6433 standard. Similarly, the compliance of railroad crossings with different distress severities to the road classification accepted in the ISO 8608 standard was investigated. As a result of all these calibrations, the levels of discomfort exposed by a passenger car travelling in urban roads at different ride speeds in double-track and single-track railroad crossings were determined with the help of dynamic vehicle model simulation that is operated in Simulink environment and can give real vehicle responses.

2. Materials and methods

2.1. Vibration analysis and equipment used

Studies have been focused on the analysis of perceived ride comfort by vibrations exposed within the vehicle and caused by the surface of the pavement. Especially when vibration measurements made in the vertical direction are made by contacting the human body, the evaluations can be analysed with the whole-body vibration (WBV) analysis approach specified in the ISO 2631 standard (ISO 1997). The first part of the standard (ISO 2631-1) describes vibration measurement and analysis methodologies. Evaluating the effects of vibrations on the human body, comfort, health, and perception analyses are performed in the frequency range of 0.5–80 Hz. Motion sickness analyses are performed in the range of 0.1–0.5 Hz (Griffin 2012).

To evaluate vibration measurements according to the response of the human body, the relative importance of the quantities (frequency, direction, etc.) of the vibration exposed must be known. For this reason, the frequency-weighted concept has been developed according to the accepted effects of the frequencies of the vibrations in a certain range. Namely, it is enlarged up to the weight value recommended by the

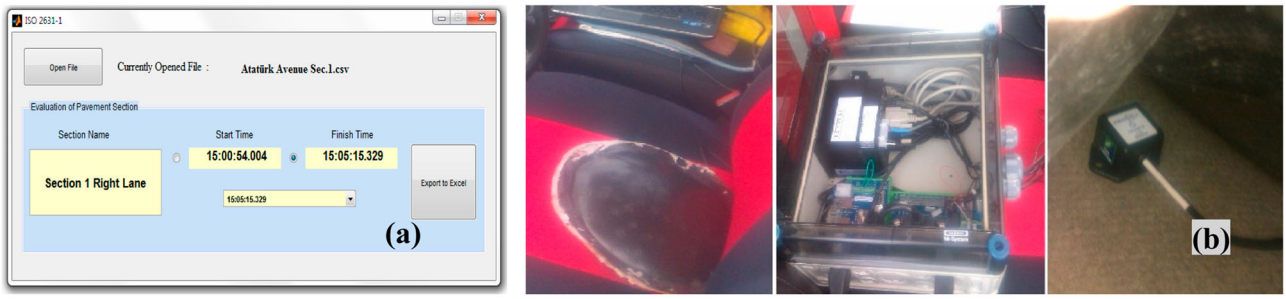

Figure 1. Vibration evaluation software interface (a) and vibration measurement set (b) used for data analysis in the study.

standard to make the human body's responses to vibrations in various frequency ranges evident (Griffin 2007).

In the ISO 2631 standard, it is recommended that vibration measurements can be made on three different axes from three different points: seat back, seat surface, and feet. From the studies conducted, it is known that the measurement point that is most effective in determining WBV is seat surface (Griffin 2007, 2012). In measurements, one of the accelerometers was placed in a particular rubber housing disc under the ischial tuberosity (Múčka 2020) to make the most accurate quantitative WBVs occur in the human body, following the directions of the ISO 2631–1 standard, EN ISO 8041 standard and ISO 10326–1 (ISO 1997, 2005, 2016).

The field measurements show that vibrations in the vertical direction (z) are the most effective in investigating the effects of the distress caused by the road surface on the human body (Zhang and Yang 2010, Duarte and de Melo 2018, Múčka 2020). Comfort concept is shown numerically with the help of the root-mean-squared (a_w) found by the frequency-weighted analysis of the measured vibration value, in the standard. Whenever this evaluation is made for vertical vibrations, it is expressed with the a_{wz} component. In the calculation of the a_{wz} component, first of all, filtered vertical acceleration ($a_{i,z}$) values, corresponding to one-third octave band intervals of the vibration signals transformed from the time domain into the frequency domain using the Butterworth filtering technique, are found. Then, these acceleration values are multiplied by the weight factor ($w_{k,\ i}$) corresponding to each band interval belonging to it. Finally, the a_{wz} component is calculated by taking the root-mean-square of these multiplications for each filtered band interval (Griffin 2007, 2012). The calculation in question can be executed mathematically using Formula (1).

$$a_{wz} = \left[\sum_i (w_{k,i}\ a_{i,z})^2\right]^{(1/2)} \quad (1)$$

Vibration measurement set designed for two accelerometers (span ±4 g, sensitivity 500 ± 15 mV/g), a GPS antenna (< 3 m accuracy) and a data logger, the vibration values in a vertical direction were recorded on the roads. Vertical vibration measurements were made with a passenger car that is in the C-segment in the 4.2 m to 4.6 m length range according to the Euro Car segment classification of passenger car type vehicles. Vertical acceleration data and GPS data were collected and transferred to the computer instantly as 1000 pcs (1000 Hz) per second and as 1 location and 1 speed per second respectively. The measured vibration values were evaluated by the researchers using the software developed in the MATLAB® interface and using the analysis method described in the ISO 2631 standard. The vibration measurement set used for field surveys and vibration evaluation software is shown in Figure 1.

In ISO 2631, when the limit values (Table 1) recommended for interpreting the vibration analysis results are examined, it is noteworthy that there is no certainty in the levels of discomfort. Since a deterministic analysis is envisaged in the study, the values found by taking the arithmetic mean of these boundaries, which are fuzzy in the interpretation of the obtained result values, were considered as discomfort limit values. This consideration is shown in Figure 2.

2.2. Railroad crossing distress

The technical standard published by ASTM with code D 6433 states that there are twenty types of distress for flexible road pavements (ASTM 2016). Among these distresses, distress 14 was identified as railroad crossing (ASTM 2016). In the standard, it is recommended that the majority of distress types be evaluated in three different distress severities, Low (L), Medium (M), and High (H). Besides, the types and severities of distress were supported with photographs to better understand the definitions and to assist the surveyors. Also, the causes of distress of pavements are divided into categories: load, climate, and other reasons. Other reasons are recognised as the cause of railroad crossing. Other reasons can be considered reasons that are beyond the control of the operator and are difficult to avoid.

In the standard, railroad crossing distress is considered as depressions or bumps around the rails, between the rails, or between the railroad lines. This type of distress is not taken into consideration if it does not cause a loss in ride comfort. It is accepted that the distress severity (L) causes a low level

Table 1. Scale of vibration discomfort suggested in ISO 2631 (ISO 1997).

a_{wz} values	Comfort level
Less than 0.315 m/s^2	Not uncomfortable
0.315–0.63 m/s^2	A little uncomfortable
0.5–1 m/s^2	Fairly uncomfortable
0.8–1.6 m/s^2	Uncomfortable
1.25–2.5 m/s^2	Very uncomfortable
Greater than 2 m/s^2	Extremely uncomfortable

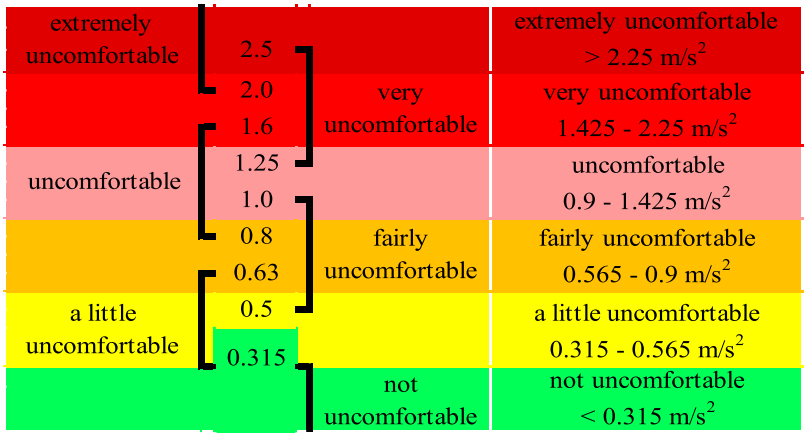

Figure 2. Considerations and limit values used in evaluating results.

of loss of ride comfort, (M) a moderate loss of ride comfort, (H) a high level of loss of ride comfort.

In this study, a large number of field observations and field measurements were examined to categorise the distress severity of double-track railroad crossings. Railroad crossings measured with guide photographs depicting the distress in the standard were compared and mutually evaluated. As a result of the investigations, it has been accepted that if the a_{wz} value, which refers to ride comfort at 30–40 km/h vehicle speeds that can be considered average urban driving speed, is less than 0.8 m/s^2, it can be considered low-severity distress, if it is in the range of 0.8–1.25 m/s^2, moderate-severity distress, and if it is greater than 1.25 m/s^2, it can be considered high-severity distress. Namely, in these speed ranges in double-track railroad crossings, it is assumed that the distress in (L) severity causes a fairly uncomfortable or more comfortable passage, the distress in (M) severity an uncomfortable passage, and the distress in (H) severity causes a passage at very uncomfortable or more severe comfort level. Samples of three railroad crossings of different severity, which were examined and measured in the light of field observations and admissions, are shown in Figure 3.

2.3. Quarter car modelling

Dynamic vehicle models are used to simulate the behaviour of a vehicle. Vehicle models consist of separate masses, springs, dampings, and shock absorbers depicting one, two, or four wheels (Agostinacchio *et al.* 2013). The quarter-car simulation concept as a pavement profile data analysis method is based on modelling the simulation of the outputs of the Bureau of Public Roads. In the light of the vehicle simulation studies conducted at the University of Michigan, it was concluded that the full-car and half-car simulation models do not provide an advantage over the quarter-car simulation models (Haas *et al.* 1994).

It is known that when modelling a quarter-car at not very high driving speeds, the tire damping effect remains at a very low level, so it can be neglected (Nguyen *et al.* 2019). Also, in the frequency-weighted vibration assessment, it was observed that there was no marginal difference between the tire-point contact model and the moving averaged profile model approaches in the numerical expression of the road profile used as an input to the dynamic vehicle model (Múčka and Gagnon 2015). Besides, the analysis shows that the difference decreases much more as the driving speed increases (Múčka and Gagnon 2015). The schematic representation and simulation parameters of the quarter-car model used in the study, which is considered to represent the vibration on the driver's seat surface are shown in Figure 4 and Table 2.

Numerical values and ratios of parameters used in vehicle modelling were determined by the values used for IRI calibration (ASTM 1997). It is possible to define mathematically the quarter vehicle simulation model used with Equations (2)–(4).

$$M_{se}\ddot{Z}se + K_{se}(Z_{se} - Z_1) + c_{se}(\dot{Z}_{se} - \dot{Z}_1) = 0 \quad (2)$$

$$M_1\ddot{Z}1 - K_{se}(Z_{se} - Z_1) - c_{se}(\dot{Z}_{se} - \dot{Z}_1) + K_1(Z_1 - Z_2) + c_1(\dot{Z}_1 - \dot{Z}_2) = 0 \quad (3)$$

$$M_2\ddot{Z}2 - K_1(Z_1 - Z_2) - c_1(\dot{Z}_1 - \dot{Z}_2) + K_2(Z_2 - Z_r) = 0 \quad (4)$$

In this study, the specified mathematical expressions were modelled in Simulink, a MATLAB® based graphic programming environment, and the results were analysed.

2.4. Artificial road profile

Superficial road elevations cause random vibrations in land vehicles moving along the road. Therefore, it is quite important to use a realistic road model when predicting a vehicle's dynamic response in advance. The profile of a road is defined as the elevation changes in the rolling surface measured on the road and parallel to the road. The ISO 8608 standard proposes a classification that corresponds to spatial frequency n_0=0.1 cycles/m and angular spatial frequency Ω_0=1 rad/m according to PSD analyses of path profile signals (ISO 1995). In the standard, eight different pavement quality classes (A, B, C, D, E, F, G, H) are proposed, using the PSD value of the road profile. Here, in terms of ride quality, Class A represents the best road and Class H represents the worst road.

Figure 3. Sample photographs of railway crossings at severity levels L (a), M (b) and H (c).

It is possible to produce an artificial road profile by using PSD analysis evaluation of road profile elevations obtained by Fourier transformation of random displacements in the standard (Du *et al.* 2020). In some studies are seen that, if the PSD function of vertical displacements is known, it is possible to create an artificial path profile by using a simple harmonic cosine function expression at an A_i amplitude and n_i spatial frequency and adding a random phase angle φ_i to a uniform probability distribution in the range 0–2π (Park *et al.* 2004, Agostinacchio *et al.* 2013). Artificial road profile can be expressed numerically by Equation (5).

$$h(x) = \sum_{i=0}^{N} A_i \cos\left(2\pi\, n_i\, x + _i\right) \tag{5}$$

In the stochastic evaluation acceptance, an artificial road profile by ISO 8608 standard can be created with Equation (6) by substituting the expression PSD of the vertical displacement instead of the amplitude (A_i) of the modified road profile signal (Agostinacchio *et al.* 2013, Du *et al.* 2020, Salmani *et al.* 2020).

$$h(x) = \sum_{i=0}^{N} \sqrt{n}\, 2^k\, 10^{-3} \left(\frac{n_0}{i\, n}\right) \cos\left(2\pi\, i\, n\, x + _i\right) \tag{6}$$

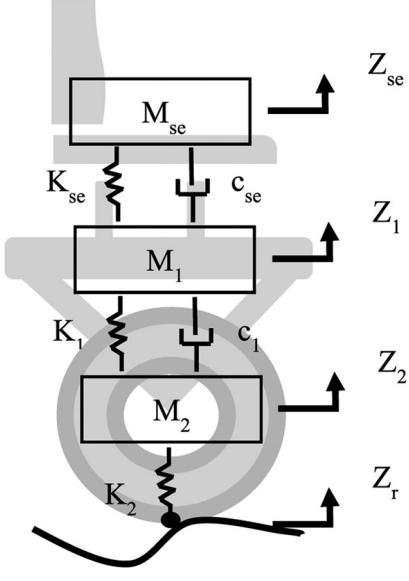

Figure 4. chematic representation of the quarter vehicle model used in the study.

In this equation, x represents the horizontal profile length from 0 to L (profile total length). Δn refers to the signal range of the profile, the total number of vertical displacement signals (points) in the N profile, i denotes the order of the signals from 0 to N. The coefficient k is a constant value that can take an integer value increasing from 3 to 9 corresponding to the road classes (actually the road pavement surface) from Class A to Class H (A, B, C, D, E, F, G, H) according to the road profile classes described in the standard. It also describes the value of n_0=0.1 cycles/m and φ_i describes the random phase angle that follows a uniform probability distribution in the 0–2π range.

3. Calibration and results

Numerical calculation methods capable of describing surface distress measurements are more successful than generalised index analysis methods (IRI, RN, etc.) in determining the ride comfort level of the pavement surface (Nguyen *et al.* 2019). It is known that artificial road (pavement) profiles are used to analyse the impact of the road surface on driving, and this method is very effective in vehicle suspension design. However, since it may not be fully sufficient to assess pavement distress and determine their impact on users, they must necessarily be calibrated with field measurements (Loprencipe and Zoccali 2017, Nguyen *et al.* 2019). At this stage of the study, the dynamic vehicle model was calibrated with vibration measurements made on-road sections with known geometry, and then the road (pavement) profile between the rails and railroad lines was characterised in railroad crossings at varied distress severity.

Table 2. Model simulation parameters.

	Model parameters	Value	Dimension
M_{se}	Seat and driver mass	110	kg
M_1	Quarter of the vehicle sprung mass	274	kg
M_2	Quarter of the vehicle unsprung mass	41.1	kg
K_{se}	Seat suspension spring stiffness	8000	N/m
K_1	Vehicle suspension spring stiffness	17344.2	N/m
K_2	Tire stiffness	178922	N/m
c_{se}	Damping ratio of the seat suspension	3000	Ns/m
c_1	Damping ratio of the vehicle suspension	1644	Ns/m
Z_r	Road input signal		
Z_1	Vertical displacement of vehicle sprung mass		
Z_2	Vertical displacement of vehicle unsprung mass		
Z_{se}	Zertical displacement of the driver's seat		

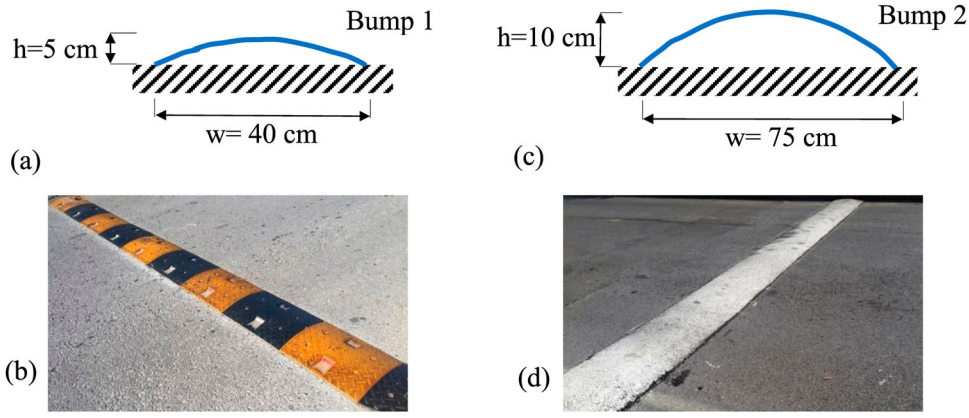

Figure 5. Geometries and images of Bump 1 (a)(b) and Bump 2 (c)(d) used in calibration of the dynamic model.

3.1. Calibration of vehicle dynamic model

The vehicle model created in the MATLAB® Simulink interface was calibrated in the study. For this purpose, vibration measurements were made with a passenger car on some road sections whose profile is known. The sections examined were determined to be a speed control bump, whose geometry is known, right in the middle of the section. Measuring distances are marked on the road surface to aid in measurements. Test sections with bumps in two different geometries were preferred to fully determine the reactions of the vehicle on different road profiles. In addition, to create the surface profile more accurately, it has been paid attention that there is no surface distresses before and after the bumps in the preferred test sections and that it is a road profile that conforms to class A according to the ISO 8608 standard. The geometries and images of the bumps on the test sections where vibration measurements are made can be seen in Figure 5.

Vibration measurements were made at a distance of five metres before and after each bump. That is, vibration measurements were repeated at 5 m + bump width + 5 m lengths and 20, 30, 40, and 50 km/h ride speeds in the test sections. Due to the presence of many factors such as environmental effects, instantaneous acceleration, and approach angle to the obstacle that will affect the vibration measurements during driving, the measurements were repeated at least three times and one of the close and meaningful ones was selected for analysis. The measured vibration data were processed with the method specified in the ISO 2631 standard, and the a_{wz} value of each measurement was calculated.

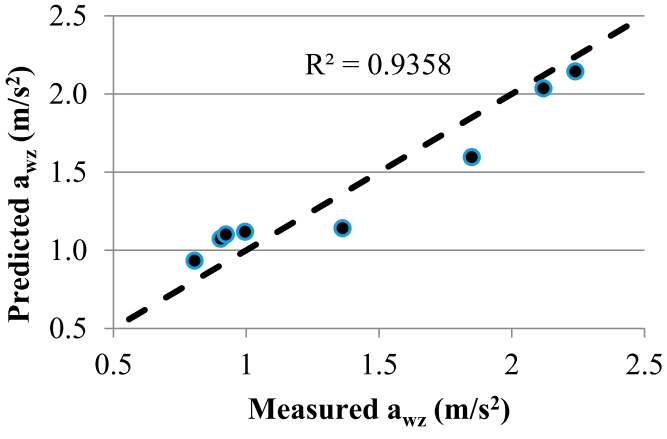

Figure 6. Comparison of a_{wz} parameters found by measurement and prediction.

Then, the profiles of these test sections were digitised using an artificial profile for the pre and post bump sections (taking the k coefficient 3), and an arc geometry for the bump section. In describing the acceleration measurement set used in the study, it was underlined that 1000 acceleration signals (1000 Hz) are read per second. Similarly, assuming that the responses of the dynamic vehicle model (see section 2.3) can be similar, in this digitisation all vertical profile elevation values are generated, depending on the measurement speed, with the profile signals being 1000 elevation values per second for the duration of the section length. Although the vehicle speeds are planned to be in integers in the calibration measurements, it was seen that these speeds differ slightly from the planned data from the GPS data recorded during the measurements. In order not to lose the accuracy of the calibration process, evaluations have been completed with the speeds recorded in the field as the measurement speed.

Vibration measurements are made from the driver's seat surface and vehicle level ground for high accuracy and control of the calibration process. All measurements were completed with a single driver weighing 80 kg. Calibration is based on the comparison of the vibrations recorded after the measurements made in the determined test sections and the vibrations obtained by simulations with the dynamic vehicle model in the time domain (Bonin *et al.* 2007, Cantisani and Loprencipe 2010). With the Matlab® Simulink software, the calculation of the constant values that help the model parameter at the determined measurement speeds has been completed by forcing the simulation to obtain the vibrations recorded on the driver's seat surface and then on the vehicle ground level.

Bumps, which are local irregularities, cause a shock acceleration to the vehicle, unlike the common disorder situation. Although there is a minimal level change before and after a hump, and yet there is a significant level change in a short distance, the model and its calibration have achieved very

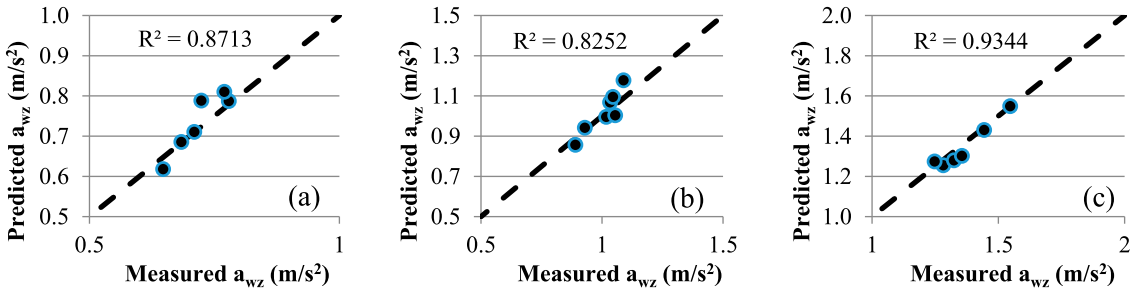

Figure 7. Comparison of L (a), M (b) and H (c) severity railroad crossing vibration parameters.

high accuracy vibration values. The regression similarity between the a_{wz} parameters found as a result of the analysis of both the vibrations measured in the field on the driver's seat surface and the vibrations simulated with the calibrated dynamic model was found to be 0.9358. This comparison can be seen in Figure 6.

3.2. Road profile according to distress severity

In the second stage of the calibration, the road profiles that could be used in the simulation were determined in the gaps between the rails and the distances outside the tracks (before and after the track and between two railroad tracks) in railroad crossings with distress severity L, M, and H. To this end, vibrations at various ride speeds were read through the driver's seat surface at crossings of a double-track railroad and a_{wz} parameter values were determined. While determining the measured section length for a double-track railroad crossing, 3.5 metres approach and departure lengths before and after the railroad tracks were accepted. These lengths are a value that indicates the largest wheelbase of a passenger car-type vehicle. The reason for choosing this value is that only railroad crossing distress is evaluated in this study. If longer distances were to be considered, it is clear that other types of distress of road pavements could be encountered. At shorter distances, it is encountered that the whole of the vibration effects that occur in the vehicle cannot be evaluated. The distance between two railroad tracks has been accepted as 3 m. This value was found by measuring in field studies where vibration data were collected. By the way, the evaluated railroad track width is normal track width and 1.5 m. It is known that grooved section rails are used in railroad crossings to provide rolling convenience to road vehicles. Since it is known that this is the case in railroad tracks that have been evaluated on the site, the profile created is modelled on a track with a grooved section about 10 cm wide. The reason is explained in this way, and the total length of the railroad crossing distress section was considered to be 13 m.

Measurements and analyses were completed on-road sections of the specified length at selected railroad crossings based on distress descriptions and distress images defined in ASTM D 6433 standard. Subsequently, road profiles at the same distances were created numerically in a computer environment. The vehicle dynamic model, which is calibrated by creating input for these road profiles, was run and the vibration values on the driver's seat surface were simulated. Since the road profiles created according to ISO 8608 are created by the principle of randomness, the same values cannot be found in each simulation result. For this reason, the predicted a_{wz} values found by the simulation were determined by running the model ten times and averaging the values found. The statistical evaluation of this simulation repeat results will be evaluated in the next part of the study.

By the results of vibration analysis, it was concluded by trial and error that it would be appropriate to select the k coefficient 5 (C road class) for the severity of L, 6 (D road class) for the k coefficient for the M severity, and 7 (E road class) for the k

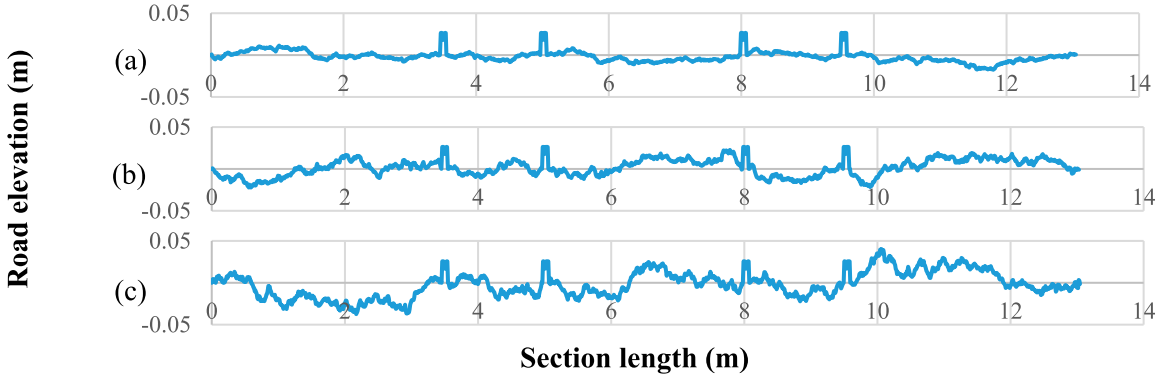

Figure 8. A double-track railroad crossing L (a), M (b), H (c) severity road profile.

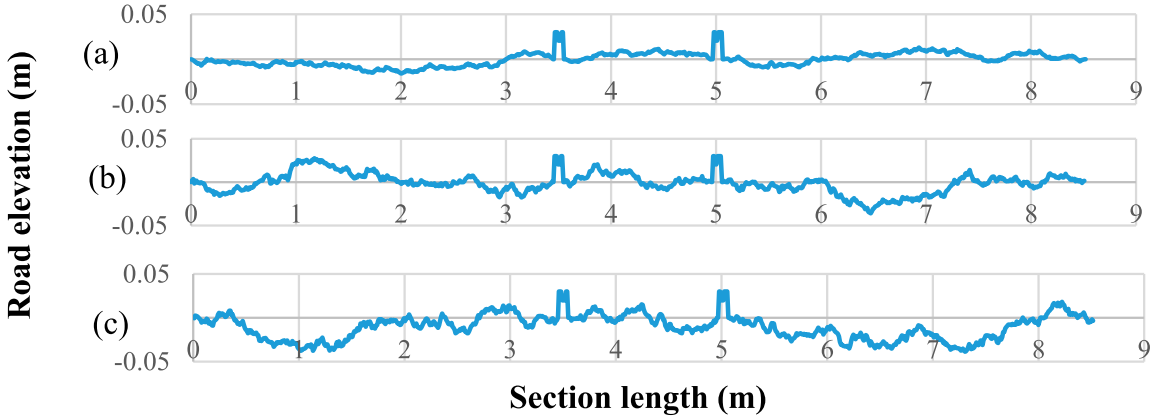

Figure 9. A single-track railroad crossing L (a), M (b), H (c) severity road profile.

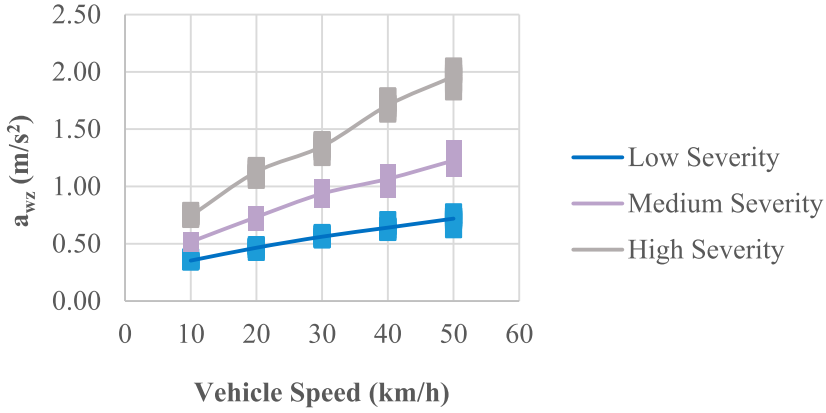

Figure 10. Data distributions as a result of a double-track railroad crossing simulation.

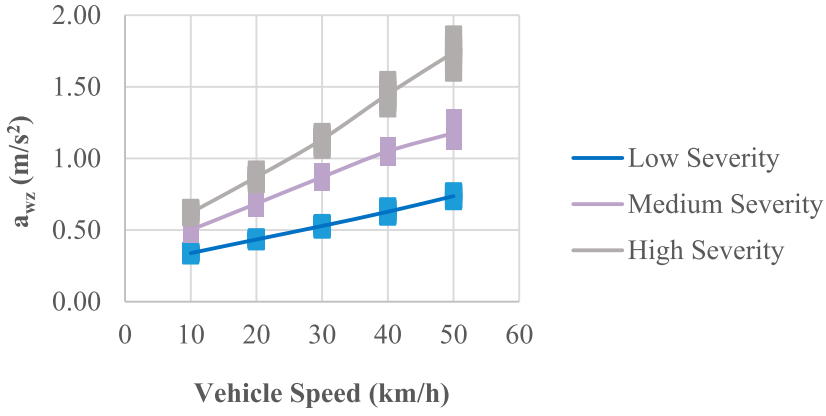

Figure 11. Data distributions as a result of a single-track railroad crossing simulation.

coefficient for the H severity. It was noticed that significant similarities could be captured when comparing the a_{wz} parameter values found as a result of the simulation with the road profiles created by selecting the relevant coefficients and the a_{wz} parameter values calculated by making field measurements. Evaluation results, regression similarities, and comparisons for three different distress severities are shown in Figure 7.

4. Ride discomfort levels and discussion

In this part of the study, the levels of discomfort encountered in double-track and single-track railroad crossing with a passenger car type vehicle were determined. Road profiles were created for double-track and single-track railroad crossing by taking into account the road class coefficients (k) determined as a result of the analyses in the previous section with the coding performed on Matlab® software. To increase understand ability,

Table 3. Standard deviation (SD) of a_{wz} data produced as a result of simulation (m/s^2).

	Double-track			Single-track		
	Low SD	Medium SD	High SD	Low SD	Medium SD	High SD
10 km/h	0.01	0.01	0.02	0.01	0.02	0.02
20 km/h	0.02	0.02	0.04	0.01	0.02	0.03
30 km/h	0.02	0.03	0.05	0.02	0.03	0.04
40 km/h	0.03	0.04	0.05	0.03	0.03	0.06
50 km/h	0.04	0.05	0.07	0.03	0.05	0.08

an example of road profiles (road profile signals) formed in double-track and single-track railroad crossing passes in each distress severity are shown in Figures 8 and 9, respectively.

As emphasised before, to determine the level of discomfort caused only by railroad crossings during riding, discomfort levels were simulated at 13 m in double-track railroad crossing and 8.5 m in single-track railroad crossing.

From the studies conducted when the literature is examined in detail, it is understood that differences of up to 17% can occur even in the measurements made with the same vehicle and at the same speed in the same pavement section in the weighted vibration analysis evaluations made with field measurement data (Múčka 2020, 2021). To simulate the real situation, road profile signals in the distances between the grooved rails were produced according to ISO 8608 in this study. As the ISO standard suggests, road profile signals are reproduced in each simulation and reflect realistically literal field conditions. This results in the generation of vibration parameters with a certain amount of deviations each time the simulation procedure works by first creating the road profile, then generating the vibration signals generated on the driver's seat surface with the vehicle dynamic responses, and finally calculating the weighted average vibration (a_{wz}) value. Therefore, in the study, the change of the resulting a_{wz} values produced by running the simulation ten times at the same ride speed with the same distress severity was observed. The largest and smallest value ranges of the simulation results data distributions of double-track and single-track railroad crossings are shown graphically in Figures 10 and 11. Also, the changes of the mean values of a_{wz} values produced in each analysis criterion are highlighted in Figures 10 and 11 as a line.

The standard deviation values for each distress severity and ride speed of the data produced as a result of simulations in

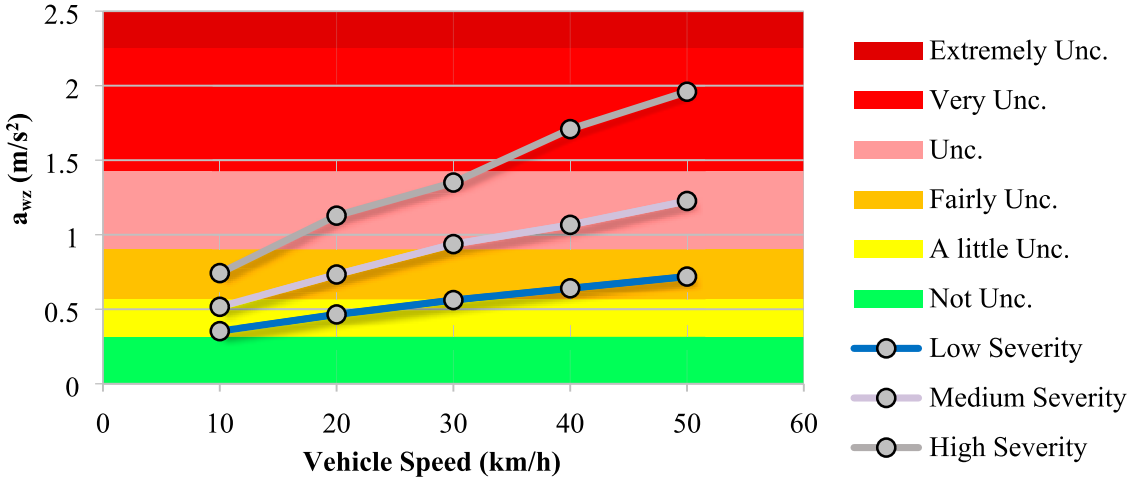

Figure 12. Graph of double-track railroad crossing discomfort thresholds.

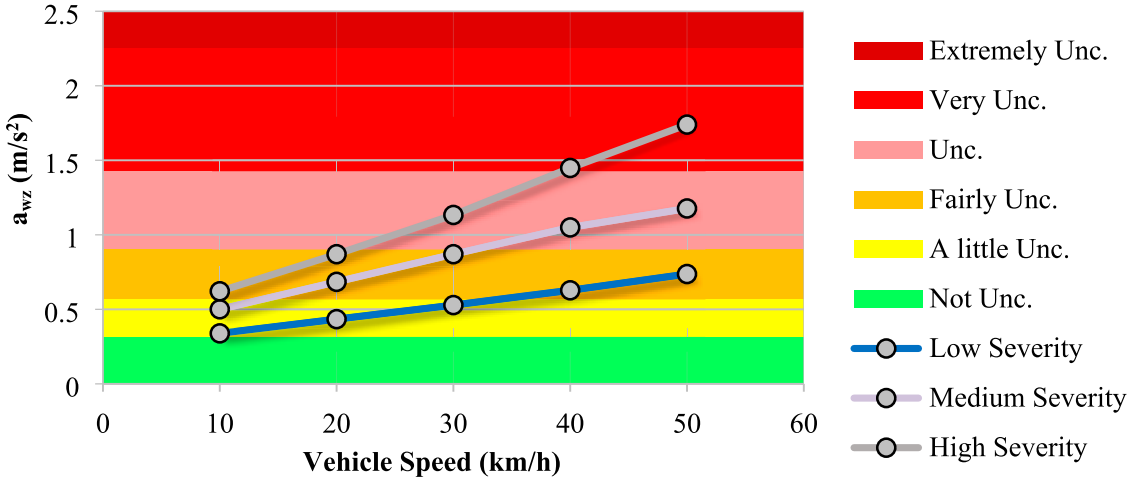

Figure 13. Graph of single-track railroad crossing discomfort thresholds.

Table 4. Railroad crossing a_{wz} discomfort threshold values (m/s^2).

	Double-track			Single-track		
	Low Sev.	Medium Sev.	High Sev.	Low Sev.	Medium Sev.	High Sev.
10 km/h	0.3529	0.5163	0.7425	0.3388	0.5003	0.6212
20 km/h	0.4652	0.7331	1.1280	0.4342	0.6846	0.8700
30 km/h	0.5614	0.9369	1.3501	0.5285	0.8699	1.1333
40 km/h	0.6405	1.0662	1.7085	0.6278	1.0496	1.4484
50 km/h	0.7193	1.2263	1.9594	0.7369	1.1769	1.7395

double-track and single-track railroad crossings are shown in Table 3. When the distribution of the simulation outputs is examined using the one-sample Kolmogorov Smirnov test statistical method, this elucidates all of the result values conform to the normal distribution in the 95% confidence interval. When the results of the standard deviation are examined, it is seen that the standard deviations of the data stacks increase with the distress severity progressing in the form of L, M, and H concerning the increase in ride speed in both railroad crossings. As the level of distress severity increases, the reason for the increase of the deviation can be explained as the increase in the profile signal randomness interval specified in the standard, in other words, the increase of the 2^k coefficient with the increase of the k value. As it is known, the path profile signal produced in the simulation was modelled as 1000 Hz to correspond to the calibration measurements. This calculation results in a decrease in the number of profile signals evaluated with the increase in speed, which leads to a decrease in the number of data and therefore an increase in the standard deviation.

The average a_{wz} vibration values changes at different driving speeds for double-track and single-track railroad crossings found as a result of the analysis are shown graphically in Figures 12 and 13, respectively. In Figures 12 and 13, the expression 'Uncomfortable' has been shortened (Unc.) due to the size limitation of the figures. Changes for speeds ranging in ten unit intervals up to 50 km/h ride speed (WHO 2015), which is used as an urban speed limit applied in many cities around the world, can be seen from the corresponding graphics, and the numerical values of the limits are shown in Table 4. In Table 4, the expression 'Severity' has been shortened (Sev.) due to the size limitation of the tables.

Pertaining to evaluation of the results, the discomfort limit values accepted within the framework of Figures 12 and 13 and Table 4 and expressed in colours in Figure 2 have been made more understandable. As understood by the colouring representation, it is seen that as distress severity increases and ride speed increases, discomfort increases in railroad crossings with passenger car. In addition to being an expected result, this situation also shows that the level of discomfort increases too much at high speeds. As can be seen from the results, a comfortable crossing (not uncomfortable) could not be provided at any speed in both types of the railroad crossing. While driving in low severity railroad crossing remains within the limits of a little uncomfortable and fairly uncomfortable, in medium severity, the uncomfortable level is also seen besides these. Clearly, driving in high severity railroad crossing cannot be more comfortable than fairly uncomfortable. Both types of the railroad crossing, ride at a high severity of 40 and 50 km/h is very uncomfortable. This indicates that the severity of distress a dramatic effect on discomfort.

5. Conclusions

The current state of road pavements can be interpreted as an indicator of the economic development level of that country (Abudinen *et al.* 2017). Pavement surface distresses are one of the most common problems in urban road networks that cause a significant amount of discomfort to drivers. In particular, the need to drive at relatively high speed due to the compelling effects of traffic (such as short green time in signalised arrangements) makes this discomfort multi-fold. In the study, the issue of the discomfort of railroad crossing pavement distress, which drivers frequently encounter in urban road networks, in two different road sections as a double-track and single-track railroad crossing, at diverse ride speeds and different distress severities, was addressed.

As part of the study, a dynamic quarter-car model that can simulate the movement of a passenger car type vehicle was created. The calibration of the model was completed with vibration measurements made in sections with two different-sized bumps. Road profiles that can be used in railway crossings with three different severity of distress were determined in areas between the tracks and outside the tracks. With this completed calibre model, the levels of discomfort experienced in urban speed limits in two different railroad crossings, namely double-track and single-track, were determined. Considering these evaluations, the following determinations were obtained.

- The level of discomfort increases too much at high speeds.
- A comfortable crossing (not uncomfortable) could not be provided at any speed in both types of the railroad crossing.
- While driving in low severity railroad crossing remains within the limits of a little uncomfortable and fairly uncomfortable, in medium severity, the uncomfortable level is also seen besides these.
- Both types of the railroad crossing, ride at a high severity of 40 and 50 km/h is very uncomfortable.
- It is seen that the discomfort increases by an average of 24% with every 10 km/h speed increase in a double-track railroad crossing. This rate is also similarly 25% in a single-track railroad crossing. These rates bring to mind that the reason increases the discomfort is the pavement areas rather than the rail crossings.
- It is understood that discomfort between 10 and 50 km/h ride speeds increased by 135% in a double-track railroad crossing, while it increased by 144% in a single-track

railroad crossing. In single-track railroad crossings, ride speed is relatively more effective on discomfort than double-track railroad crossings.

In this study, the adverse effects of railroad crossings, which are frequently encountered in urban road networks, on ride comfort are expressed in numerical values. The vital importance of keeping railway crossings well maintained on ride comfort has been pointed out. It is aimed to give an idea to the organisations operating the road pavement in decision-making. It is recommended that discomfort can be determined for different vehicle types in the later stages of the study.

Disclosure statement

No potential conflict of interest was reported by the author(s).

References

Abudinen, D., Fuentes, L.G., and Carvajal Muñoz, J.S, 2017. Travel quality assessment of urban roads based on international roughness index. *Transportation Research Record: Journal of the Transportation Research Board*, 2612, 1–10.

Agostinacchio, M., Ciampa, D., and Olita, S, 2013. The vibrations induced by surface irregularities In road pavements – a matlab® approach. *European Transport Research Review*, 6 (3), 267–275.

Astarita, V., *et al*., 2012. A mobile application for road surface quality control: uniqualroad. *Procedia - Social and Behavioral Sciences*, 54, 1135–1144.

ASTM, 1997. *Standard practices for simulating vehicular response to longitudinal profiles of traveled surface. ASTM E 1170-97*. West Conshohocken, PA: ASTM International.

ASTM, 2016. *Standard practice for roads and parking lots pavement condition index surveys. ASTM D 6433-16*. West Conshohocken, PA: ASTM International.

Bonin, G., *et al*., 2007. Ride quality evaluation: 8 d.O.F. Vehicle model calibration. *4th International SIIV Congress*. Palermo, Italy.

Bridgelall, R, 2015. Precision bounds of pavement distress localization with connected vehicle sensors. *Journal of Infrastructure Systems*, 21 (3), 04014045.

Cantisani, G., and Loprencipe, G, 2010. Road roughness and whole body vibration: evaluation tools and comfort limits. *Journal of Transportation Engineering*, 136 (9), 818–826.

Du, H., *et al*., 2020. *Advanced seat suspension control system design for heavy duty vehicles, 1st ed*. London, UK: Academic Press.

Duarte, M.L.M., and De Melo, G.C., 2018. Influence of pavement type and speed on whole body vibration (wbv) levels measured on passenger vehicles. *Journal of the Brazilian Society of Mechanical Sciences and Engineering*, 40 (3), 150.

Fuentes, L., *et al*., 2021. Pavement serviceability evaluation using whole body vibration techniques: A case study for urban roads. *International Journal of Pavement Engineering*, 22 (10), 1238–1249.

Griffin, M.J, 2007. Discomfort from feeling vehicle vibration. *Vehicle System Dynamics*, 45 (7-8), 679–698.

Griffin, M.J, 2012. *Handbook of human vibration*. London, UK: Academic press.

Guanyu, W., Michael, B., and Gurmel, G, 2020. Study of the factors affecting road roughness measurement using smartphones. *Journal of Infrastructure Systems*, 26 (3), 04020020.

Haas, R., Hudson, W.R., and Zaniewski, J.P., 1994. *Modern pavement management*. Malabar, FL: Krieger Pub. Co.

Hou, X., *et al*., Year. The analysis of the correlation between international roughness index and body ride comforted.^eds. *Ninth International Conference of Chinese Transportation Professionals (ICCTP)*, Harbin, China: American Society of Civil Engineers (ASCE), 2554-2561.

ISO, 1995. *Mechanical vibration - road surface profiles - reporting of measured data. ISO 8608*. Geneva, Switzerland: ISO.

ISO, 1997. *Mechanical vibration and shock - evaluation of human exposure to whole-body vibration, part 1: general requirement. ISO 2631-1*. Geneva, Switzerland: ISO.

ISO, 2005. *Human response to vibration - measuring instrumentation. ISO BS EN 8041*. Geneva, Switzerland: ISO.

ISO, 2016. *Mechanical vibration — laboratory method for evaluating vehicle seat vibration — part 1: basic requirements. ISO 10326-1*. Geneva, Switzerland: ISO.

Janani, L., Sunitha, V., and Mathew, S, 2020. Influence of surface distresses on smartphone-based pavement roughness evaluation. *International Journal of Pavement Engineering*, 22 (13), 1637–1650.

Kırbaş, U., and Karaşahin, M, 2016. Performance models for hot mix asphalt pavements In urban roads. *Construction and Building Materials*, 116, 281–288.

Kırbaş, U., and Karaşahin, M, 2018a. Investigation of ride comfort limits on urban asphalt concrete pavements. *International Journal of Pavement Engineering*, 19 (10), 949–955.

Kırbaş, U., and Karaşahin, M, 2018b. Pavement performance levels causing human health risks. *Journal of the Croatian Association of Civil Engineers*, 70 (10), 851–861.

Kırbaş, U., and Karaşahin, M, 2019. Determination of pavement performance thresholds for comfortable riding on urban roads. *Journal of Testing and Evaluation*, 47 (1), 20170319.

La Torre, F., Ballerini, L., and Di Volo, N., 2002. Correlation between longitudinal roughness and user perception In urban areas. *Transportation Research Record*, 1806 (1), 131–139.

Loprencipe, G., and Zoccali, P, 2017. Ride quality due to road surface irregularities: comparison of different methods applied on a set of real road profiles. *Coatings*, 7 (59), 1–16.

Múčka, P, 2015. Sensitivity of road unevenness indicators to distresses of composite pavements. *International Journal Pavement Research Technology*, 8 (2), 72–84.

Múčka, P, 2017. Road roughness limit values based on measured vehicle vibration. *Journal of Infrastructure Systems*, 23 (2), 04016029.

Múčka, P, 2020. Vibration dose value In passenger car and road roughness. *Journal of Transportation Engineering, Part B: Pavements*, 146 (4), 1–15, 04020064.

Múčka, P, 2021. International roughness index thresholds based on whole-body vibration In passenger cars. *Transportation Research Record*, 2675 (1), 305–320.

Múčka, P., and Gagnon, L, 2015. Influence of tyre–road contact model on vehicle vibration response. *Vehicle System Dynamics*, 53 (9), 1227–1246.

Muniz De Farias, M., and De Souza, R.O., 2009. Correlations and analyses of longitudinal roughness indices. *Road Materials and Pavement Design*, 10 (2), 399–415.

Nguyen, T., *et al*., 2019. Bus ride index – a refined approach to evaluating road surface irregularities. *Road Materials and Pavement Design*, 22 (2), 423–443.

Park, S., Popov, A.A., and Cole, D.J, 2004. Influence of soil deformation on off-road heavy vehicle suspension vibration. *Journal of Terramechanics*, 41 (1), 41–68.

Salmani, H., *et al*., 2020. A new criterion for comfort assessment of In-wheel motor electric vehicles. *Journal of Vibration and Control*, 1–13.

Sauerwein, P.M., and Smith, B.L., 2011. *Investigation of the implementation of a probe-vehicle based pavement roughness estimation system*. Final Report, University of Virginia Center for Transportation Studies, Charlottesville, VA, UVA-2010-01.

Vittorio, A., *et al*., 2014. Automated sensing system for monitoring of road surface quality by mobile devices. *Procedia - Social and Behavioral Sciences*, 111, 242–251.

Wang, F., and Easa, S, 2016. Analytical evaluation of ride comfort on asphalt concrete pavements. *Journal of Testing and Evaluation*, 44 (4), 1671–1682.

Who, 2015. *Global status report on road safety*. Italy: Organization. W.H., WA 275.

Yu, J., Chou, E.Y.J., and Yau, J.-T, 2006. Development of speed-related ride quality thresholds using international roughness index. *Transportation Research Record: Journal of the Transportation Research Board*, 1974, 47–53.

Zhang, J., *et al*., 2020. Iri threshold values based on riding comfort. *Journal of Transportation Engineering, Part B: Pavements*, 146 (1), 04020001.

Zhang, H., and Yang, W, 2010. Evaluation method of pavement roughness based on human-vehicle-road interaction. *Icctp 2010.* 3541-3551.